Mining of Mineral Deposits
Volume 20 (2026), Issue 1, 28-40

MMD JOURNAL / MINING.IN.UA

https://doi.org/10.33271/mining20.01.028

Environmental geological assessment of naturally occurring asbestos based on mineralogical and spatial analysis: The Bajgora-Mitrovicë Area, Kosovo

Bahri Sinani [1], Blazo Boev [2], Arianit Reka [3,4], Berat Sinani [2], Ivan Boev [2*]

[1] *Department of Environmental Engineering, Faculty of Natural and Technical Science, University "Goce Delchev", Shtip, North Macedonia*
[2] *Department of Petrology, Mineralogy and Geochemistry, Faculty of Natural and Technical Science, University "Goce Delchev", Shtip, North Macedonia*
[3] *Department of Chemistry, Faculty of Natural Sciences and Mathematics, University of Tetova, Tetovo, North Macedonia*
[4] *Albanian Unit of Nanoscience and Nanotechnology, NanoAlb, Academy of Sciences of Albania, Tirana, Albania*

**Corresponding author: e-mail ivan.boev@ugd.edu.mk*

Abstract

Purpose. To evaluate the spatial distribution and mineralogical variability of naturally occurring asbestos (NOA) in the Bajgora region and assess its environmental significance in relation to geological conditions and current land-use patterns, to identify asbestos-bearing zones and provide a spatial basis for environmental hazard assessment.

Methods. A combined mineralogical, statistical, and geospatial approach was applied. Twenty representative rock samples were collected across the study area and analyzed using X-ray powder diffraction (XRD) and scanning electron microscopy coupled with energy-dispersive X-ray spectroscopy (SEM-EDX) to identify and quantify asbestos-related mineral phases. Descriptive statistics, correlation analysis, and principal component analysis (PCA) were used to evaluate mineralogical variability and phase associations. Spatial interpolation using Kriging was performed in GIS software to visualize the distribution of serpentine-group minerals and chrysotile and to support environmental hazard zoning.

Findings. The results indicate pronounced mineralogical heterogeneity within the Bajgora region, dominated by serpentine-group minerals, including lizardite (with multiple polytypes), antigorite, and subordinate chrysotile. Lizardite is the most widespread phase, reflecting low-temperature serpentinization, whereas antigorite locally dominates under higher-temperature, higher-pressure conditions. Chrysotile occurs discontinuously and is spatially restricted to specific structural zones, such as fracture systems and lithological contacts. Statistical and multivariate analyses confirm non-random spatial patterns and strong geological control on mineral distribution.

Originality. This study provides one of the first integrated mineralogical-statistical-spatial assessments of NOA in the Bajgora region, linking detailed phase characterization with spatial modeling to support site-specific environmental risk evaluation in ophiolitic terrains of the Western Balkans.

Practical implications. The generated spatial distribution maps provide a practical tool for environmental risk zoning, land-use planning, and prioritizing monitoring and mitigation measures in areas affected by naturally occurring asbestos.

Keywords: *naturally occurring asbestos; chrysotile; serpentine minerals; spatial analysis; environmental hazard zoning*

1. Introduction

Asbestos is a group of naturally occurring fibrous silicate minerals widely used in industrial applications for their high thermal resistance, tensile strength, and chemical stability. However, extensive epidemiological and toxicological studies have demonstrated that inhalation of airborne asbestos fibers is associated with severe long-term health effects, including asbestosis, lung cancer, and malignant mesothelioma. As a result, the use of asbestos has been strictly regulated or banned in many countries, while environmental and public health concerns related to asbestos exposure remain highly relevant [1]-[4].

Mineralogically, asbestos minerals are divided into two major groups: serpentine and amphibole asbestos. Chrysotile, a serpentine-group mineral, represents the most widespread form of asbestos globally and is commonly associated with serpentinized ultramafic rocks. In many ophiolitic complexes, chrysotile occurs together with other serpentine minerals, such as lizardite and antigorite, reflecting different stages and physicochemical conditions of serpentinization. These mineralogical associations are critical for understanding the spatial variability, stability, and environmental behavior of asbestos-bearing rocks [4].

In recent decades, attention has shifted from anthropogenic asbestos-containing materials to naturally occurring asbestos (NOA), hosted by ultramafic, mafic, and related lithologies. In areas underlain by serpentinites and other ultrabasic rocks, asbestos fibers may be released into the environment through natural weathering or anthropogenic ground disturbance, including excavation, road construction,

Received: 8 October 2025. Accepted: 6 February 2026. Available online: 30 March 2026

Mining of Mineral Deposits. ISSN 2415-3443 (Online) | ISSN 2415-3435 (Print)

quarrying, mining, and infrastructure development. Such processes create a direct pathway from geological occurrence to potential human exposure, particularly in regions experiencing active land-use change [5].

Effective management of NOA-related environmental hazards requires not only the mineralogical identification of asbestos-bearing phases but also spatially explicit information on their distribution and relationships with geological structures, lithological boundaries, and human activity. Spatial analysis and hazard zoning approaches are therefore increasingly recognized as essential tools for assessing potential exposure and supporting evidence-based land-use planning and risk mitigation strategies [6], [7]. Similar spatially oriented approaches have been successfully applied in environmental and geological risk assessments, where geospatial analysis and zoning techniques have been used to identify areas of increased hazard and support decision-making [8]. Advances in environmental information technologies further enhance the integration of geological data with spatial models for risk evaluation [9].

The Bajgora region, located in northern Kosovo within the Vardar Zone, represents a geologically complex area characterized by widespread ophiolitic units and serpentinized ultramafic rocks. In recent years, the region has undergone accelerated infrastructure development and tourism expansion, including road construction and the development of residential and recreational facilities [10]. These activities increase the likelihood of ground disturbance within asbestos-bearing terrains and highlight the need for integrated geological and environmental assessments to support sustainable regional development and public health protection. The application of GIS-based data processing, optimization techniques, and spatial modeling has been widely used in geoscientific studies to enhance the reliability of subsurface and environmental assessments [11]-[14].

The objective of this study is to evaluate the spatial distribution and mineralogical variability of NOA-related mineral phases in the Bajgora region and to translate these data into applied products for environmental assessment. Specifically, the study aims to characterize asbestos-bearing mineral assemblages using mineralogical methods, analyze their spatial distribution in relation to geological and structural controls, and delineate zones of increased environmental hazard and potential exposure under present-day land-use conditions [1], [10], [15]. The resulting mineralogical, statistical, and spatial models provide a basis for environmental hazard zoning, risk communication, and prioritization of monitoring and mitigation measures in areas affected by naturally occurring asbestos [1], [2], [4], [5], [10], [15].

2. Study area

The Vardar Zone is a central tectonic unit formed during the geodynamic evolution of the Alpine-Mediterranean orogenic system. It is commonly subdivided into the Western, Central, and Eastern Vardar zones [16]-[17][18]. It comprises an extensive ophiolitic belt separating the Serbian-Macedonian Massif from the Dinarides and represents a contact zone between oceanic and continental lithospheric segments [19]-[22].

The Bajgora region is situated within the Vardar Zone in northern Kosovo (Fig. 1) [23]. Its western part belongs to the Western Vardar Subzone, whereas the eastern part is associated with the Central and Eastern Vardar subzones [1], [17], [18]. These subzones differ in their stratigraphic and structural characteristics. In particular, Upper Cretaceous flysch deposits interact with ophiolitic sequences of the Western Subzone, reflecting a complex tectono-sedimentary evolution [18]. The Bajgora-Kaçandol belt represents a distinct tectonic unit within the Vardar Zone and is closely linked to the southern structural systems of this domain [1], [23], [24].

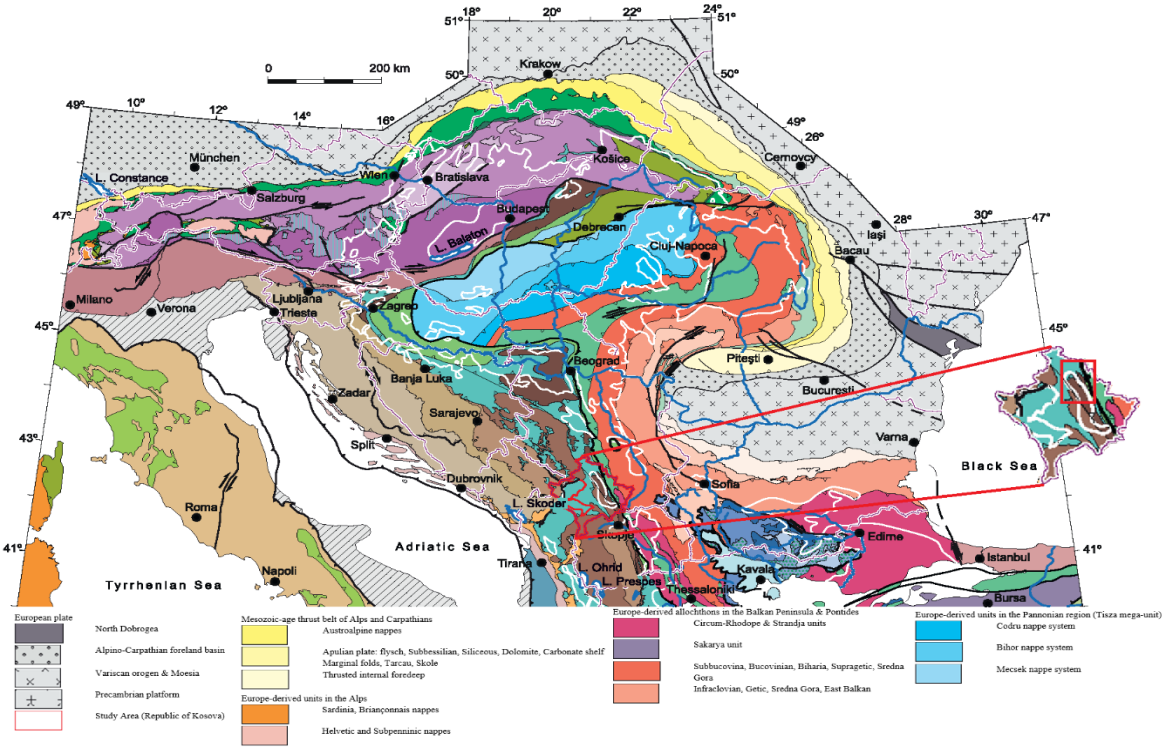

Figure 1. Tectonic framework of the Alpine collision zone between the Eastern Alps and western Turkey, showing the position of the Vardar Zone and the location of the study area in northern Kosovo

Geologically, the study area is characterized by the predominance of ophiolitic complexes and associated sedimentary units (Fig. 2). Jurassic serpentinites are tectonically overlain by Cretaceous limestones, marls, conglomerates, and sandstone flysch sequences [1], [10], [20], [25], [26]. Contacts between serpentinized ultrabasic rocks and carbonate formations are vital, as they represent favorable zones for the development of naturally occurring asbestos (NOA) mineralization [1], [27], [28].

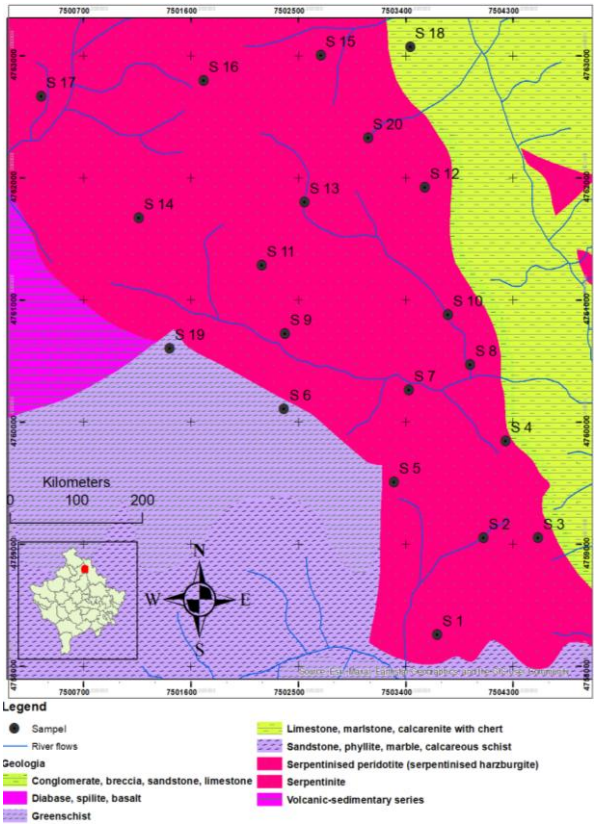

Figure 2 Geological map of the study area (scale 1:25000), showing the distribution of ophiolitic units, sedimentary formations, and sampling locations

Ultrabasic rocks in Kosovo are known to host mineralization of asbestos, chromium, and talc [29]. The Mitrovica region, especially the Bajgora Mountains, is one of the most significant areas with documented NOA occurrences, with estimated reserves of approximately 8.9 million tons [29]-[31]. Although the geological occurrence of NOA in this region has been investigated in several studies, integrated approaches combining mineralogical data with spatial and statistical analysis for site-specific environmental risk assessment remain limited, particularly in the Western Balkans. The present study addresses this gap by linking mineralogical characterization with spatial analysis to support environmental hazard zoning in complex ophiolitic terrains.

3. Materials and methods

3.1. Analytical methods and spatial data processing

Rock samples were collected across the study area and analyzed using X-ray Powder Diffraction (XRPD) and Scanning Electron Microscopy coupled with Energy-Dispersive X-ray Spectroscopy (SEM/EDX) to identify and characterize asbestos-bearing mineral phases [32].

To accurately represent the spatial distribution of asbestos and assess environmental risks, the study employed ArcMap 10.7 and Golden Software Surfer, integrating data from field surveys, GPS measurements, and laboratory analyses [33], [34]. This approach enabled the creation of a spatial database used for zoning and mapping of asbestos distribution and environmental hazard levels [35].

The results of the spatial analysis were used to develop an environmental hazard map that highlights zones with varying degrees of potential environmental risk [1], [36], [37]. In addition, a social vulnerability map was produced to identify areas where local populations and visitors are most physically exposed to asbestos-related risks. Asbestos distribution was mapped using Golden Software Surfer to identify zones of varying environmental risk [38].

3.2. Field data collection and ancillary information

The first phase of the study comprised systematic field investigations, including geological observations of lithological units, documentation of asbestos-bearing occurrences, and compilation of statistical data related to the surveyed settlements [29]. In parallel, information on land-use patterns, such as construction activities, tourism development, agriculture, and livestock farming, was collected, as these factors are directly linked to surface disturbance and potential pathways of asbestos exposure [30].

Historical sources indicate that the study area was exploited for asbestos mineral extraction before World War II. Remnants of former mining activities, including asbestos-containing tailings and landfill sites, are still preserved in the field and were documented during field surveys (Fig. 3) [29].

Figure 3. Remnants of asbestos-containing tailings and landfill sites in the Bajgora region are associated with historical mining activities since the 1940s

3.3. Geological and structural sampling

Rock sampling was carried out across the study area following an approximately uniform spatial scheme, taking into account the availability and accessibility of bedrock surface exposures (Fig. 4) [39]. For each sampling location, geographic coordinates were recorded using a handheld GPS receiver, ensuring accurate spatial positioning within the KosRef coordinate system. During field sampling, lithological, structural, and morphological characteristics of the exposed rocks were documented, and a unique identification code was assigned to each collected sample [39].

A total of 20 rock samples were collected. Nineteen samples were identified as containing fibrous mineral phases. They were preliminarily classified based on their color, texture, and morphological features, whereas one sample exhibited distinct mineralogical composition and structural characteristics compared to the others.

Following laboratory analyses, spatial evaluation of the sampling results was performed in ArcGIS 10.7 and web-based mapping tools to assess the distribution patterns of fibrous minerals and support environmental risk mapping.

(a)

(b)

Figure 4. Field evidence of asbestos-bearing serpentinites in the Bajgora area: (a) structurally fractured serpentinite with asbestos-bearing zones; (b) close-up view of fibrous mineral aggregates observed in serpentinite outcrops (photo: B. Sinani)

3.4. Geological and structural sampling

Collected rock samples were transported to the University of Mitrovica's laboratory for physical preparation before mineralogical and microscopic analyses. Each sample was first crushed and ground in a Pin Yan mill until a fine, homogeneous granulometry was achieved. The ground material was subsequently sieved, and the fraction with a particle size ≤ 63 µm was selected for further analysis [40].

From the ≤ 63 µm fraction, 10 g of material was weighed for each sample and packaged under controlled conditions to ensure consistency between samples and to minimize contamination or material loss (Fig. 5) [15], [31].

Figure 5. Prepared rock samples after grinding and sieving to a particle size of ≤ 63 µm and weighing 10 g for laboratory analyses

This fraction was considered suitable for XRPD and SEM/EDX analyses based on standard mineralogical preparation protocols. Given the inherent heterogeneity of rock samples, including variable grain size, surface roughness, and mineral distribution, particular attention was paid to obtaining representative subsamples and reducing potential sources of analytical bias during preparation [41], [42].

3.5. Laboratory analyses

Prepared samples were analyzed at Zonguldak Bülent Ecevit University (Zonguldak, Turkey). Micromorphological and mineralogical investigations were conducted using a field-emission scanning electron microscope (FE-SEM; FEI Quanta FEG 450). Observations were performed in backscattered electron (BSE) mode under low-vacuum conditions, using an accelerating voltage in the range of 15-20 kV (Fig. 6). This configuration was selected to enhance atomic number contrast and to facilitate the identification of asbestiform mineral phases based on their morphological characteristics [32].

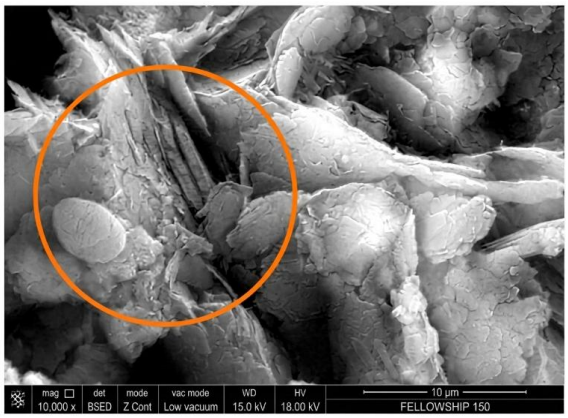

Figure 6. Laboratory identification of asbestos-bearing phases (SEM-BSE micrograph)

Mineralogical characterization was further supported by X-ray powder diffraction (XRPD) analysis. The obtained diffraction patterns were processed and interpreted using the Rietveld refinement method, allowing reliable identification and quantitative estimation of crystalline phases present in the samples [43]. The combined use of SEM-based observations and XRPD analysis enabled robust identification of asbestos-related mineral phases, including chrysotile, within the analyzed samples.

4. Results and discussion

4.1. Spatial distribution of mineralogical phases

The mineralogical composition of each sampling point is visualized using cylindrical charts, allowing direct comparison of phase proportions between individual localities. Figure 7 presents the spatial distribution of asbestos-bearing mineral phases derived from mineralogical analyses of georeferenced field samples. The map integrates the relative abundances of antigorite, lizardite, and chrysotile, which represent the dominant serpentine-group minerals occurring within the ultrabasic rocks of the study area. Such variability is characteristic of heterogeneous serpentinization pathways and textural evolution of ultramafic rocks controlled by fluid-rock interaction processes, as described in classical studies on serpentine textures and serpentinization [44].

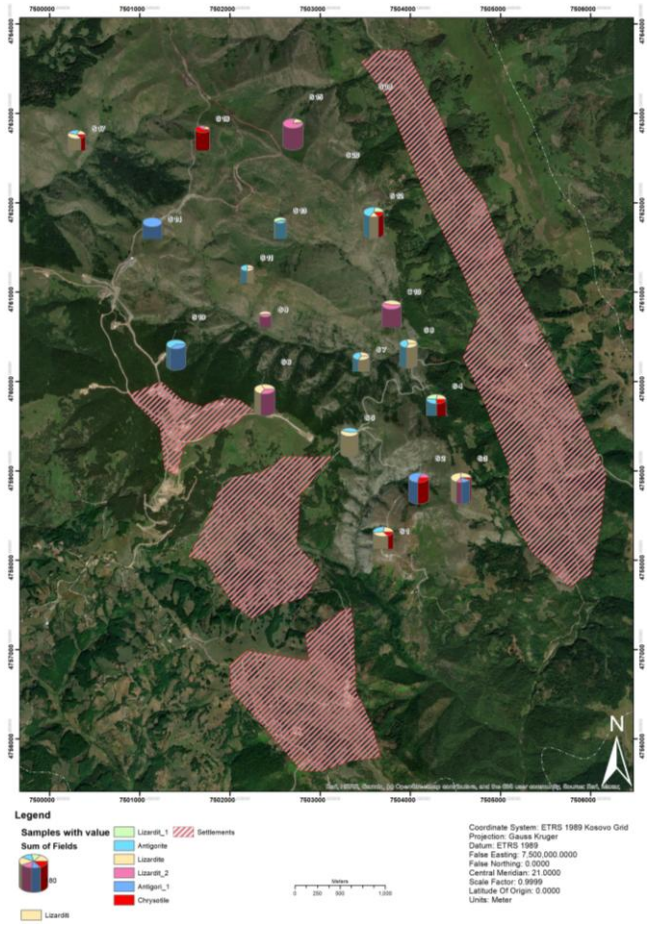

Figure 7. Spatial distribution of asbestos-bearing minerals based on the mineralogical composition of the analyzed samples

Among the identified phases, chrysotile, the principal asbestiform mineral, is the most critical factor from an environmental risk perspective. In contrast, antigorite and lizardite, although generally considered less hazardous, are included to illustrate the petrogenetic framework and mineralogical evolution of the serpentinized ultramafic units. The map also shows the spatial distribution of nearby settlements, enabling a preliminary evaluation of potential population exposure. In several locations, chrysotile-bearing samples occur in proximity to inhabited areas, which increases the environmental sensitivity of these zones.

The spatial patterns of serpentine-group minerals and chrysotile, identified by X-ray diffraction (XRD), exhibit pronounced variability across the study area. These variations reflect differences in the degree of serpentinization, structural controls, and local geological conditions that influence the formation and preservation of asbestiform mineral phases.

Radial diagrams were used to visualize the relative distribution of the analyzed mineral phases across the sampled locations (Fig. 8a-g). This graphical representation enables direct comparison of relative phase proportions across individual sampling points and highlights spatial variability associated with local geological and alteration conditions.

The distribution of antigorite (Fig. 8b) shows localized maxima, most prominently at samples S7 and S10, indicating a heterogeneous spatial pattern within the study area. Such enrichment suggests variations in serpentinization intensity and structural control, commonly associated with hydrothermal alteration zones where antigorite is stable under relatively higher pressure and moderate temperature conditions.

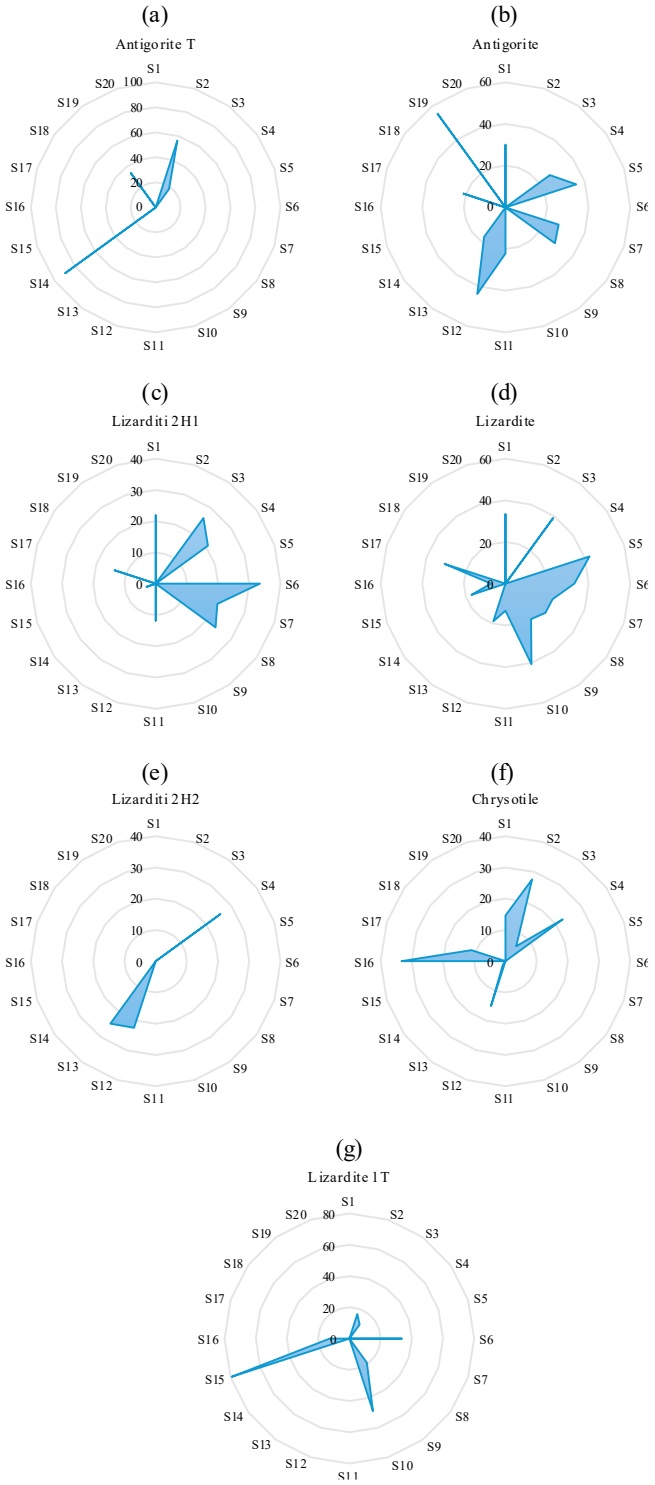

Figure 8. Radial diagrams illustrating the relative distribution of mineralogical phases across the sampled locations: (a) antigorite T; (b) antigorite; (c) lizardite 2H1; (d) lizardite; (e) lizardite 2H2; (f) chrysotile; (g) lizardite 1T

Antigorite T (Fig. 8a) generally exhibits low values and a more restricted spatial distribution, without clearly dominant concentration zones, indicating that this variant represents a minor, locally developed phase formed under specific physicochemical conditions.

The radial diagrams for lizardite and lizardite 2H1 (Fig. 8d, c) reveal contrasting spatial behaviors. Lizardite (Fig. 8d) shows a comparatively broader distribution, with pronounced concentration peaks at samples S6, S9, and S10,

consistent with low-temperature serpentinization processes affecting ultramafic rocks. In contrast, lizardite 2H1 (Fig. 8c) displays a more fragmented and spatially restricted pattern, with elevated values primarily confined to samples S2 and S7, suggesting formation under localized crystallization conditions and micro-scale variations in physicochemical parameters.

The distributions of lizardite 2H2, chrysotile, and lizardite 1T (Fig. 8e-g) further emphasize the heterogeneity of serpentine mineral phases within the study area. Lizardite 2H2 (Fig. 8e) exhibits a minimal distribution, with a pronounced concentration observed only at sample S11, indicating that this polytype is relatively uncommon and associated with spatially constrained geothermal or physicochemical conditions. Chry-sotile (Fig. 8f), the most environmentally relevant asbestiform phase, shows distinct concentration peaks at samples S3 and S15. Its uneven and localized distribution suggests strong control by discrete geological or structural factors, and the occurrence of elevated chrysotile content at isolated sampling points warrants critical consideration in environmental risk assessment. Lizardite 1T (Fig. 8g) displays a scattered distribution with localized enrichments, reflecting additional variability in serpentinization pathways and crystallization environments. This spatially restricted occurrence is consistent with the metastable nature of chrysotile, which forms and persists only under specific physicochemical and structural conditions and is readily transformed under changing temperature-pressure regimes [2].

4.2. Mineralogical composition and statistical characteristics of samples

Mineralogical compositions of the analyzed samples, determined by X-ray diffraction (XRD), are summarized in Table 1. The results indicate pronounced variability in the occurrence and relative abundance of serpentine-group minerals across samples S1-S20. The assemblage is dominated by serpentine minerals, including multiple polytypes of lizardite, two forms of antigorite, and subordinate chrysotile, which are characteristic of serpentinized ultramafic rocks.

Table 1. Mineralogical composition of samples from the Bajgora region based on X-ray diffraction (XRD) analysis

Sample	X	Y	Z	Antigorite t	Antigorite	Lizarditi 2H1	Lizardite	Lizarditi 2H2	Chrysotile	Lizardite 1T
S1	7503699	4758173	1274	0.0	30.1	21.9	33.4	0.0	14.6	0.0
S2	7504095	4758987	1293	56.1	0.0	0.0	0.0	0.0	27.5	16.4
S3	7504563	4758989	1343	18.2	0.0	26.0	38.9	0.0	5.9	11.1
S4	7504287	4759799	1183	0.0	26.4	20.7	0.0	25.6	22.7	0.0
S5	7503326	4759456	1347	0.0	35.8	0.0	42.5	0.0	0.0	0.0
S6	7502385	4760067	1470	0.0	0.0	33.4	33.1	0.0	0.0	33.5
S7	7503456	4760225	1351	0.0	26.9	20.8	23.8	0.0	0.0	0.0
S8	7503981	4760440	1490	0.0	29.4	23.7	23.7	0.0	0.0	0.0
S9	7502393	4760698	1320	0.0	0.0	0.0	21.0	0.0	0.0	19.1
S10	7503792	4760859	1234	0.0	0.0	0.0	40.6	0.0	0.0	48.9
S11	7502193	4761271	1549	0.0	22.1	11.8	12.9	0.0	0.0	0.0
S12	7503594	4761926	1349	0.0	43.7	0.0	18.9	22.4	15.1	0.0
S13	7502559	4761803	1392	0.0	17.5	0.0	0.0	24.7	1.4	0.0
S14	7501139	4761670	1610	89.5	0.0	0.0	0.0	0.0	0.0	0.0
S15	7502699	4763034	1509	0.0	0.0	3.5	17.2	0.0	0.0	79.3
S16	7501695	4762824	1436	0.0	0.0	0.0	7.0	0.0	33.3	12.6
S17	7500300	4762691	1174	0.0	21.8	14.2	30.8	0.0	11.5	0.0
S18	7503467	4763106	1482	0.0	0.0	0.0	0.0	0.0	0.0	0.0
S19	7501403	4760576	1495	33.9	56.0	0.0	0.0	0.0	0.0	0.0
S20	7503105	4762342	1472	0.0	0.0	0.0	0.0	0.0	0.0	0.0

Lizardite occurs in significant proportions in several samples (S1, S3, S6, S8, S10, and S15), reaching approximately 49%, whereas it is absent in other locations. This heterogeneous distribution suggests spatially non-uniform serpentinization, strongly controlled by local geological factors such as structural setting, hydrothermal fluid circulation, and the degree of alteration of the parent ultramafic rocks [45]. The coexistence of different lizardite polytypes (2H1, 2H2, and 1T) reflects multiple crystallization stages, primarily driven by variations in temperature and pressure during the area's geological evolution. The occurrence of lizardite 1T and 2H1 polytypes is consistent with their distinct crystal structures and stability fields reported in crystallographic studies of serpentine minerals [46]. Similar multistage mineral transformation processes, controlled by changing physicochemical conditions, have been documented in other mineral systems, including sulfide-bearing ores, highlighting the general role of temperature, fluid composition, and reaction pathways in mineral phase evolution [47].

Antigorite is present in high proportions in selected samples (S2, S14, S15, and S19), reaching ~80-90%, indicating near-total dominance of this phase in specific zones. Such enrichment is indicative of higher-temperature conditions and a more advanced stage of serpentinization, consistent with the established thermodynamic stability field of antigorite [2], [48]. These mineralogical patterns confirm that the study area comprises distinct geological micro-environments with contrasting thermal regimes and alteration histories, accounting for the observed compositional heterogeneity.

Chrysotile, the most environmentally and health-relevant asbestiform phase, was identified in a limited number of samples (S1, S2, S12, S16, and S17), with abundances ranging from low to moderate. Its restricted and discontinuous occurrence suggests formation under highly localized structural conditions, such as fracture networks or deformation zones that act as preferential pathways for fluid-assisted fiber growth [45]-[48]. Descriptive statistical parameters calculated for the mineralogical phases are presented in Table 2.

Mean, median, and modal values of zero across several phases indicate intermittent occurrence and a discontinuous spatial distribution.

Antigorite and antigorite T exhibit the highest variance and standard deviation, reflecting firm spatial heterogeneity and clustered distributions influenced by geological factors such as hydrothermal alteration and tectonic control. In contrast, lizardite 2H2 shows lower variability, suggesting a more homogeneous, limited distribution. Chrysotile is characterized by relatively low mean values but a high coefficient of variation, indicating localized enrichment despite its overall limited presence. Statistical parameters, including mean values, 95% confidence intervals, and results of the t-test, are summarized in Table 3.

Table 2. Descriptive statistical parameters of serpentine-group mineral phases identified in the analyzed samples

Parameter	Antigorite	Antigorite T	Lizarditi 2H1	Lizardite	Lizarditi 2H2	Chrysotile	Lizardite 1T
Mean	15.49	9.89	8.8	17.19	3.64	6.6	11.05
Median	8.75	0	0	18.05	0	0	0
Mode	0	0	0	0	0	0	0
Standard deviation	17.76	23.71	11.47	15.65	8.89	10.56	20.87
Variance	315.39	562.3	131.49	245.02	79.1	111.55	435.68
Coefficient of variation	1.15	2.4	1.3	0.91	2.45	1.6	1.89
Minimum	0	0	0	0	0	0	0
Maximum	56	89.5	33.4	42.5	25.6	33.3	79.3
Range	56	89.5	33.4	42.5	25.6	33.3	79.3
Interquartile range	27.53	0	20.73	31.38	0	12.28	13.55
Skewness	0.72	2.64	0.83	0.21	2.14	1.49	2.36
Kurtosis	-0.5	6.79	-0.86	-1.46	2.89	1.1	5.67

Table 3. Statistical parameters (mean values, 95% confidence intervals, t-test results, and p-values) for the studied mineralogical phases

Parameter	Antigorite T	Antigorite	Lizarditi 2H1	Lizardite	Lizarditi 2H2	Chrysotile	Lizardite 1T
Mean	9.89	15.49	8.80	17.19	3.64	6.60	11.05
Lower CI (95%)	-1.21	7.17	3.43	9.86	-0.53	1.66	1.28
Upper CI (95%)	20.98	23.80	14.17	24.52	7.80	11.54	20.81
±CI (Half-width)	11.10	8.31	5.37	7.33	4.16	4.94	9.77
t-stat	1.864	3.899	3.432	4.911	1.828	2.795	2.366
p-value	0.0778	0.0010	0.0028	0.0001	0.0833	0.0116	0.0287

The analysis was performed by testing the null hypothesis (H_0 mean = 0) for each mineralogical phase using a two-sided test. The phases lizardite 2H1, antigorite, lizardite, lizardite 1T, and chrysotile exhibit statistically significant results ($p < 0.05$), with confidence intervals that do not include zero, indicating non-random occurrence and statistically stable mean values. In contrast, lizardite 2H2 and antigorite T do not reach the 95% significance level ($p > 0.05$), and their confidence intervals include zero, suggesting higher uncertainty and less consistent spatial occurrence.

Overall, the statistical results support the interpretation that lizardite and antigorite represent the dominant and more stable serpentine phases within the study area. In contrast, their 2H2 and T variants are less consistently developed and spatially restricted. The high coefficients of variation observed for most phases confirm substantial heterogeneity and justify the application of spatial interpolation and mapping techniques in subsequent analyses.

4.3. Skewness and kurtosis analysis

The relationship between skewness and kurtosis for the mineralogical phases identified in the investigated area is illustrated in Figure 9. Skewness describes the degree of asymmetry of the data distribution relative to the mean, whereas kurtosis reflects the concentration of values around the mean and the weight of distribution tails. Each bar represents a specific mineral phase, highlighting differences in statistical distribution patterns and variability among the analyzed serpentine minerals. The skewness values shown in Figure 9 indicate that several mineral phases exhibit asymmetric distributions. Lizardite 2H1 and lizardite 2H2 display negative skewness, indicating distributions with longer tails toward lower values and a tendency for concentrations to cluster toward higher values.

In contrast, antigorite and lizardite 1T show pronounced positive skewness, reflecting distributions dominated by lower values with occasional high-concentration outliers. Chrysotile and antigorite T exhibit slightly positive skewness, suggesting moderately asymmetric but relatively balanced distributions. The kurtosis results further emphasize differences in distribution characteristics among the mineral phases. Most phases are characterized by negative kurtosis (platykurtic distributions), indicating flatter distributions with a broader spread of values and reduced clustering around the mean. Lizardite 2H2 and antigorite T exhibit the lowest kurtosis values, suggesting particularly high variability and dispersed concentration patterns. In contrast, antigorite shows slightly positive kurtosis, indicating a more peaked distribution and greater concentration around the mean, approaching normality.

Overall, the combined skewness and kurtosis patterns reflect substantial mineralogical heterogeneity within the study area and support the interpretation that spatially variable geological and physicochemical conditions control the occurrence of serpentine mineral phases.

4.4. Correlation matrix of mineralogical phases

The Pearson correlation matrix presented in Table 4 provides insight into the statistical relationships between the concentrations of serpentine-group mineral phases identified by XRD analysis. The correlation coefficients (r) describe the degree and direction of linear association between pairs of mineral phases, allowing evaluation of potential co-occurrence patterns and contrasting formation conditions.

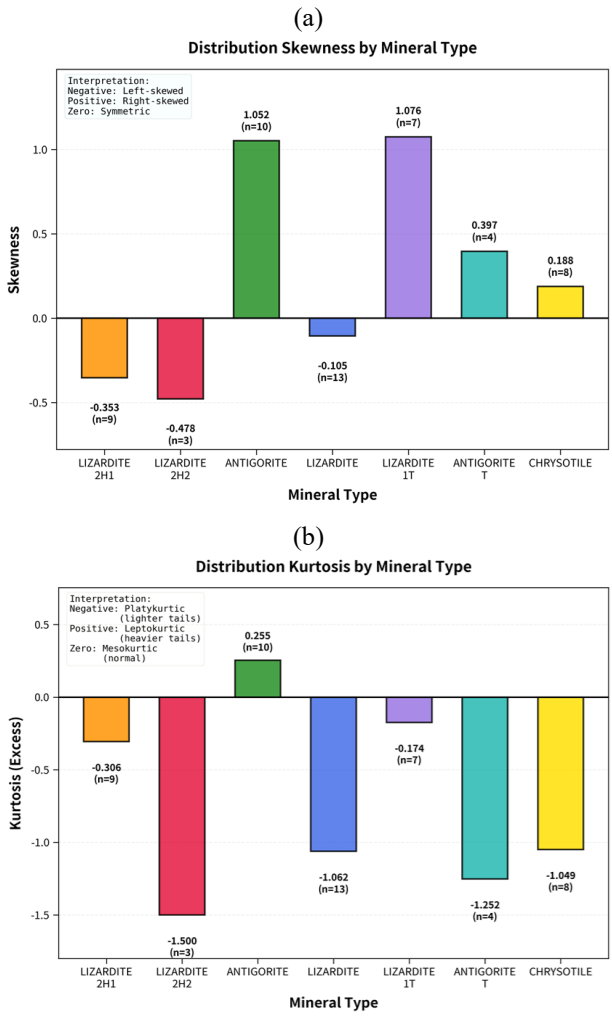

Figure 9. Skewness and kurtosis of serpentine-group mineral phases identified in the analyzed samples: (a) skewness; (b) kurtosis

A moderate positive correlation is observed between lizardite 2H1 and lizardite ($r = 0.45$), indicating a tendency for these two phases to occur together within the analyzed samples. This relationship is consistent with the development of lizardite polytypes under similar low- to moderate-temperature serpentinization conditions, where comparable physicochemical environments favor their co-crystallization.

A weak to moderate correlation is identified between lizardite 2H2 and antigorite ($r = 0.32$), as well as between lizardite 2H2 and chrysotile ($r = 0.27$). These associations suggest partial overlap of petrological conditions during hydrothermal alteration, where localized variations in temperature, pressure, and fluid composition may permit the formation of multiple serpentine phases within restricted zones.

In contrast, a moderate to strong negative correlation is observed between lizardite and antigorite ($r = -0.49$), as well as between lizardite 1T and antigorite ($r = -0.49$). These inverse relationships reflect the contrasting stability fields of these mineral phases: antigorite typically forms under higher pressure-temperature conditions, whereas lizardite is characteristic of serpentinites formed at lower metamorphic grades.

Additionally, antigorite T shows a moderate negative correlation with lizardite ($r = -0.38$) and weak correlations with most other phases. This pattern is consistent with the limited, spatially restricted occurrence of antigorite T observed in the study area and suggests that more specific, localized physicochemical conditions control its formation.

Overall, the correlation matrix highlights the coexistence and mutual exclusivity of serpentine mineral phases within the study area, supporting the interpretation that spatially variable serpentinization processes and contrasting thermal regimes play a key role in controlling mineralogical assemblages.

The results of the Principal Component Analysis (PCA) are summarized in Table 5, which presents the loadings of the mineralogical phases for the first five principal components.

Table 4. Pearson correlation matrix for serpentine-group mineral phases identified in the analyzed samples

Variable	Lizarditi 2H1	Lizarditi 2H2	Antigorite	Lizardite	Lizardite 1T	Antigorite T	Chrysotile
Lizarditi 2H1	1	–	–	–	–	–	–
Lizarditi 2H2	-0.06	1	–	–	–	–	–
Antigorite	0.08	0.32	1	–	–	–	–
Lizardite	0.45	-0.31	0.06	1	–	–	–
Lizardite 1T	-0.06	-0.23	-0.49	0.25	1	–	–
Antigorite T	-0.25	-0.18	-0.15	-0.38	-0.11	1	–
Chrysotile	-0.02	0.27	-0.02	-0.22	-0.12	0.07	1

Table 5. Principal Component Analysis (PCA) loadings for the mineralogical phases identified in the analyzed samples

Variable	DIM.1	DIM.2	DIM.3	DIM.4	DIM.5
Lizarditi 2H2	0.695	0.207	0.451	-0.386	0.21
Antigorite	0.571	0.605	-0.337	0.096	0.319
Lizardite	-0.579	0.615	-0.022	0.396	0.193
Lizardite 1T	-0.73	-0.134	0.455	-0.212	0.387
Antigorite T	0.143	-0.77	-0.449	0.108	0.386
Chrysotile	0.446	-0.273	0.588	0.612	0.024

These components describe the main directions of variability in the dataset and reflect contrasting associations among the serpentine-group minerals.

The first principal component (Dim.1) is primarily controlled by opposing contributions of lizardite and lizardite 1T (negative loadings) versus lizardite 2H2 and antigorite (positive loadings). This contrast indicates a differentiation between lizardite-dominated assemblages and those enriched in antigorite and related polytypes, reflecting differences in mineral structure and textural development.

The second principal component (Dim.2) emphasizes the contrast between antigorite and lizardite (positive loadings) and between antigorite T and antigorite (strong negative loading). This pattern suggests variability across different serpentinization pathways or physicochemical conditions that affect the stability of antigorite variants relative to lizardite phases.

The third and fourth components (Dim.3 and Dim.4) highlight the contribution of chrysotile, which exhibits relatively high positive loadings, together with selected lizardite polytypes. These dimensions, therefore, capture the variability in the occurrence of the asbestiform phase and its relationship with specific serpentine polymorphs.

The fifth component (Dim.5) shows more evenly distributed and generally lower loadings, indicating a minor contribution to the overall variance and reflecting secondary variability within the dataset.

Overall, the PCA results reveal complex relationships among serpentine mineral phases and confirm that multiple mineralogical associations coexist within the study area. These patterns support the interpretation that spatially variable serpentinization processes and contrasting physicochemical conditions have governed the development of the observed mineral assemblages.

The eigenvalues and the percentage of variance explained by the principal components are summarized in Table 6, demonstrating the effectiveness of PCA in reducing the dataset's dimensionality while preserving its essential variability. The first three principal components (PC1-PC3) account for approximately 74% of the total variance, indicating that a limited number of components captures the dominant mineralogical variability. The first two components (PC1 and PC2) together explain 56.16% of the variance, reflecting the influence of the leading mineralogical associations and structural controls. Including the fourth component increases the cumulative explained variance to over 86%, further improving the dataset's representation. The three-dimensional PCA score plot based on the first three components (Dim.1-Dim.3) is presented in Figure 10.

Table 6. Eigenvalues and percentage of variance explained by each principal component derived from the PCA

PC	Eigenvalue	Percent_variance	Cumulative_percent
PC1	1.9	31.61	31.61
PC2	1.47	24.55	56.16
PC3	1.07	17.86	74.02
PC4	0.75	12.42	86.44
PC5	0.48	8.04	94.48
PC6	0.33	5.52	100

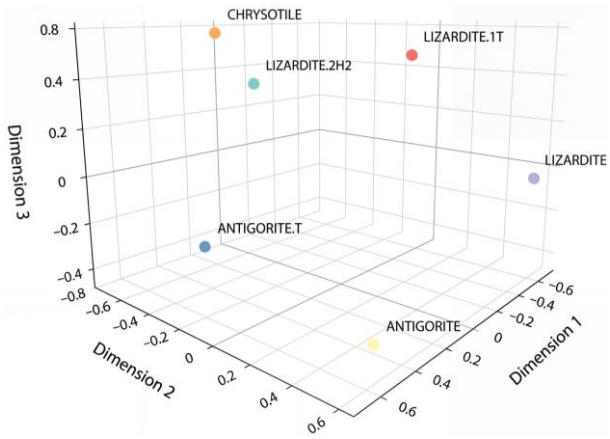

Figure 10. Three-dimensional principal component analysis (PCA) score plot based on the first three components (Dim.1-Dim.3)

This representation, interpreted in conjunction with the component loadings (Table 5) and the explained variance (Table 6), reveals a clear separation among the main serpentine mineral phases, highlighting the strong mineralogical and structural control over the data's variability.

In the PCA space, chrysotile and lizardite 1T are positioned at positive values of Dim.3, consistent with their high loadings on this component and indicating their distinct contributions to the overall variance. In contrast, antigorite and antigorite T are primarily differentiated along Dim.1 and Dim.2, which together explain more than half of the total variance. This separation reflects contrasting mineralogical assemblages and transformation pathways within the serpentinized ultramafic rocks.

These relationships are consistent with the Pearson correlation analysis, which indicates weak to moderate correlations between selected mineral phases, such as lizardite-lizardite 2H1 and antigorite-lizardite 1T, suggesting partial coexistence under overlapping but not identical physicochemical conditions. Overall, the combined results of PCA and correlation analysis confirm that the observed mineralogical variability is primarily controlled by lizardite polymorphism and progressive transformations toward antigorite and chrysotile, reflecting spatially variable serpentinization processes within the study area.

4.5. Spatial distribution of mineralogical phases in the Bajgora region

Spatial analysis of the distribution of serpentine-group mineral phases was performed in Golden Software Surfer using the Kriging interpolation method to visualize the spatial variability of mineral concentrations across the study area. The interpolated surfaces represent relative concentration patterns derived from georeferenced sampling points and provide insight into the influence of lithological heterogeneity and structural controls on mineral distribution [49], [50].

The three-dimensional spatial models illustrate pronounced spatial differentiation among the analyzed mineral phases (Fig. 11a-g). These patterns reflect the combined effects of ultramafic lithology, serpentinization intensity, tectonic structures, and localized hydrothermal alteration processes.

Antigorite (Fig. 11a) is predominantly concentrated in the northern and northeastern sectors of the study area, where two distinct concentration maxima are observed. This distribution suggests a strong structural control, potentially related to tectonic zones that facilitated fluid circulation and promoted higher-temperature serpentinization.

In contrast, antigorite T (Fig. 11b) exhibits a more restricted and discontinuous distribution, with localized concentration peaks in the northwestern and eastern parts of the area. The isolated nature of these maxima indicates that they formed under specific, spatially limited physicochemical conditions.

The spatial distributions of lizardite 2H1 and lizardite 2H2 further emphasize the heterogeneity of serpentinization processes (Fig. 11c, d). Lizardite 2H1 shows two principal concentration zones in the central-western and eastern parts of the study area, suggesting formation within localized alteration zones, possibly linked to Mg-rich fluid circulation. In contrast, lizardite 2H2 displays a fragmented spatial pattern, with elevated concentrations confined to limited areas, indicating sensitivity to small-scale lithological variability and locally advanced alteration conditions.

Dominant concentrations in the central and northeastern sectors of the study area characterize Lizardite 1T (Fig. 11e). The presence of two major distribution peaks suggests an association with contact zones between ultramafic and mafic rock units, where chemical and physical conditions favored the stability of this polytype.

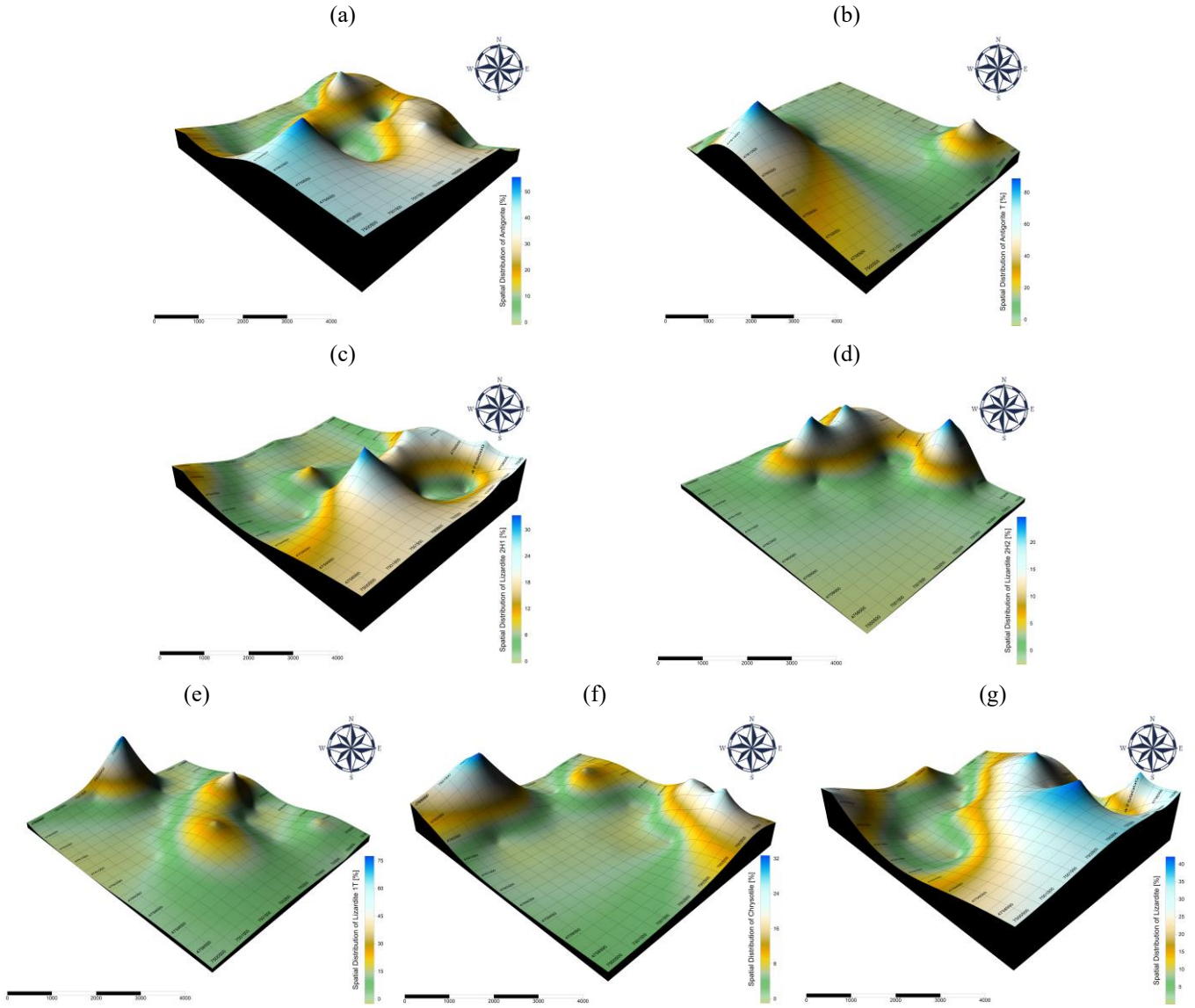

Figure 11. Three-dimensional spatial distribution of serpentine-group mineral phases in the Bajgora region derived from Kriging interpolation: (a) antigorite; (b) antigorite T; (c) lizardite 2H1; (d) lizardite 2H2; (e) lizardite 1T; (f) chrysotile; (g) lizardite

The spatial distribution of chrysotile (Fig. 11f) is notably uneven, with several localized high-concentration zones. The most pronounced peaks occur in the northeastern and southeastern parts of the study area, whereas the central and western sectors exhibit comparatively lower values. This pattern indicates that chrysotile mineralization is not continuous but restricted to specific geological micro-environments, commonly associated with fracture systems, lithological contacts, and zones of enhanced deformation that provide favorable conditions for fiber growth.

Finally, the distribution of total lizardite (Fig. 11g) reflects a broader and more continuous spatial pattern compared to individual lizardite polytypes. Elevated concentrations are mainly observed in the central and northeastern parts of the study area, indicating that lizardite represents the dominant serpentine phase formed under widespread low-temperature serpentinization conditions. This distribution supports the interpretation of extensive fluid-rock interaction during the early stages of ultramafic rock alteration.

The spatial models demonstrate that the distribution of serpentine minerals and chrysotile in the Bajgora region is highly fragmented and structurally controlled. The concentration patterns correspond closely with tectonic features, lithological boundaries, and alteration zones, confirming that lithological heterogeneity and tectonic activity play a decisive role in controlling the occurrence of asbestos-related minerals. Given the proximity of several high-concentration zones to areas of tourism and human activity, these spatial patterns represent an important basis for environmental hazard assessment and risk mitigation planning. Consequently, the identified spatial relationships highlight the necessity of integrating mineralogical data with land-use and infrastructure information to improve the reliability of site-specific environmental risk assessments.

5. Conclusions

The results of this study demonstrate that the Bajgora region is characterized by favorable geological conditions for the formation and spatial development of naturally occurring asbestos (NOA). Mineralogical analyses based on X-ray diffraction (XRD) and SEM-EDX investigation of 20 representative samples indicate that the ultramafic rocks of the area are dominated by serpentine-group minerals, including lizardite (with several polytypes), antigorite, and subordinate chrysotile.

Lizardite represents the most abundant mineral phase, reaching concentrations of approximately 40-50% in several samples. Its heterogeneous spatial distribution reflects low-temperature serpentinization processes, controlled by variable fluid circulation intensity and local geological conditions. The identification of multiple lizardite polytypes (2H1, 2H2, and 1T) indicates multistage crystallization, associated with changes in temperature and pressure during serpentinization.

Antigorite dominates in selected locations, where its abundance exceeds 50%, suggesting formation under relatively higher temperature and pressure conditions than those for lizardite. These variations confirm the presence of distinct serpentinization regimes within the study area.

Chrysotile, the mineral phase of most significant environmental concern due to its asbestiform nature, occurs in only a limited number of samples and generally at moderate concentrations. Its restricted and discontinuous distribution indicates formation under localized structural conditions, such as fracture systems and lithological contacts, that favor the development and preservation of fibrous minerals.

The combined statistical, multivariate, and spatial analyses reveal pronounced mineralogical heterogeneity, primarily controlled by the degree of serpentinization and polymorphic transformations within the serpentine group. While lizardite and antigorite exhibit more continuous regional distributions, chrysotile is confined to localized zones, commonly associated with tectonic structures, representing areas of elevated environmental and public health concern.

Spatial interpolation using the Kriging method highlights a fragmented distribution of mineral phases across the Bajgora region. Antigorite is mainly concentrated in the northern and northeastern sectors, and lizardite predominates in the central part of the study area. In contrast, chrysotile shows localized concentration peaks near tectonic lineaments and lithological contacts.

From an environmental perspective, chrysotile-bearing zones represent areas of increased risk, particularly as human activity and land use grow. Therefore, the spatial distribution maps produced in this study provide a robust basis for environmental risk zoning, supporting the development of targeted monitoring, land-use planning, and mitigation strategies in the Bajgora region.

Author contributions

Conceptualization: BaS, IB; Data curation: AR; Formal analysis: BaS, BB, BeS; Investigation: BaS, BeS; Methodology: BB, AR; Resources: AR; Software: BeS; Supervision: IB; Validation: AR, IB; Visualization: AR; Writing – original draft: BaS, BeS; Writing – review & editing: BB, IB. All authors have read and agreed to the published version of the manuscript.

Funding

This research received no external funding.

Acknowledgements

The authors would like to thank the Editor and the reviewers for their constructive comments and suggestions, which significantly improved the quality of the manuscript.

Conflicts of interest

The authors declare no conflict of interest.

Data availability statement

The original contributions presented in the study are included in the article, further inquiries can be directed to the corresponding author.

References

[1] Sinani, B., Boev, B., Reka, A.A., Sinani, B., & Boev, I. (2025). Distribution of naturally occurring asbestos in the Mitrovica region: Geochemical and mineralogical characterization. *Geosciences*, *15*(9), 335. https://doi.org/10.3390/geosciences15090335

[2] Evans, B.W. (2004). The serpentinite multisystem revisited: Chrysotile is metastable. *International Geology Review*, *46*(6), 479-506. https://doi.org/10.2747/0020-6814.46.6.479

[3] Raimbekova, A., Kapralova, V., Popova, A., Kubekova, S., Dalbanbay, A., Kalenova, A., Mustahimov, B., Yermekbayeva, S., & Myrzabekova, S. (2024). Corrosion behavior of mild steel in sodium sulfate solution in presence of phosphates of different composition. *Journal of Chemical Technology and Metallurgy*, *59(*2), 367-377. https://doi.org/10.59957/jctm.v59.i2.2024.16

[4] Viirta, R.L. (2006). Worldwide asbestos supply and consumption trends from 1900 through 2003. *Circular*, *1298*, 80. https://doi.org/10.3133/cir1298

[5] Wilk, E., Krówczyńska, M., & Zagajewski, B. (2019). Modelling the spatial distribution of asbestos-cement products in Poland with the use of the random forest algorithm. *Sustainability*, *11*(16), 4355. https://doi:10.3390/su11164355

[6] Kezembayeva, G., Rysbekov, K., Dyussenova, Z., Zhumagulov, A., Umbetaly, S., Barmenshinova, M., Yerkezhan, B., & Zhakypbek, Y. (2025). Public health risk assessment of quantitative emission from a molybdenum production plant: Case study of Kazakhstan. *Engineered Science*, *34*, 1454. https://doi.org/10.30919/es1454

[7] Bekbassarov, S., Soltabaeva, S., Daurenbekova, A., & Ormanbekova, A. (2015). "Green" economy in mining. *New Developments in Mining Engineering*, 431-434. https://doi.org/10.1201/b19901-75

[8] Shults, R., Seitkazina, G., Annenkov, A., Demianenko, R., Soltabayeva, S., Kozhayev, Z., & Orazbekova, G. (2025). Complex geodetic monitoring of the massive sports structures by terrestrial laser scanning. *Civil Engineering Journal*, *11*(3), 884-909. https://doi.org/10.28991/CEJ-2025-011-03-05

[9] Baimukhanbetova, E., Onaltayev, D., Daumova, G., Amralinova, B., & Amangeldiyev, A. (2020). Improvement of informational technologies in ecology. *E3S Web of Conferences*, *159*, 01008. https://doi.org/10.1051/e3sconf/202015901008

[10] Meholli, B. (2014). *Ophiolitic magmatism and new magmatism in the Bajgora region, mineral resources associated with them*. PhD Dissertation. Tiranë, Albania: Polytechnic University of Tirana.

[11] Nazirova, A., Kalimoldayev, M., Abdoldina, F., & Dubovenko, Y. (2022). Optimization of an information system module for solving a direct gravimetry problem using a genetic algorithm. *Eastern-European Journal of Enterprise Technologies*, *2*(9(116)), 21-34 https://doi.org/10.15587/1729-4061.2022.253976

[12] Abdoldina, F.N., Nazirova, A.N., Dubovenko, Y.I., & Umirova, G.K. (2020). On the solution of the gravity direct problem for a prism with a simulated annealing approach. *Geomodel 2020*, *1*, 1-5. https://doi.org/10.3997/2214-4609.202050014

[13] Dubovenko, Y.I., Nazirova, A.B., & Abdoldina, F.N. (2022). Data-driven preprocessing of gravity data in oilfield GIS monitoring system in Kazakhstan. *International Conference Monitoring of Geological Processes and Ecological Condition of the Environment*, *1*, 1-4. https://doi.org/10.3997/2214-4609.2022580267

[14] Abdoldina, F., Nazirova, A., Dubovenko, Y., & Umirova, G. (2020). On the solution of the gravity direct problem for a sphere with a simulated annealing approach. *International Multidisciplinary Scientific GeoConference*, *20*(2.1), 239-245. https://doi.org/10.5593/sgem2020/2.1/s07.031

[15] Adu, S.A., Gyang, P.A., & Yakin, Z. (2025). The role of GIS and spatial analysis in enhancing urban resilience and disaster response for vulnerable US communities. *World Journal of Advanced Research and Reviews*, *27*(1), 746-754. https://doi.org/10.30574/wjarr.2025.27.1.2567

[16] Toljić, M., Stojadinović, U., & Krstekanic, N. (2019). Vardar zone: New insights into the tectono-depositional subdivision. *II Geological Congress of Bosnia and Herzegovina*, 60-73.

[17] Bilalli, B., Gawlick, H.J., Prela, M., & Uta, A. (2025). *Ophiolitic mélanges in southeastern Kosovo*. Tiranë, Albania: Polytechnic University of Tirana.
[18] Hengl, T. (2007). *A practical guide to geostatistical mapping of environmental variables* (EUR 22904 EN). Office for Official Publications of the European Communities. Retrived from: https://publications.jrc.ec.europa.eu/repository/handle/JRC38153
[19] Zelic, M., Marroni, M., Pandolfi, L., & Trivić, B. (2010). Tectonic setting of the Vardar suture zone (Dinaric-Hellenic belt): The example of the Kopaonik area (Southern Serbia). *Ofioliti*, *35*(1), 49-69.
[20] Robertson, A.H.F., & Karamata, S. (1994). The role of subduction-accretion processes in the tectonic evolution of the Mesozoic Tethys in Serbia. *Tectonophysics*, *234*(1-2), 73-94. https://doi.org/10.1016/0040-1951(94)90205-4
[21] Ahmadi, H., Hussaini, M.R., Yousufi, A., Bekbotayeva, A., Baisalova, A., Amralinova, B., Mataibayeva, I., Rahmani, A.B., Pekkan, E., & Sahak, N. (2023). Geospatial insights into ophiolitic complexes in the Cimmerian realm of the Afghan Central Block (Middle Afghanistan). *Minerals*, *13*(11), 1453. https://doi.org/10.3390/min13111453
[22] Robertson, A.H., Trivić, B., Đerić, N., & Bucur, I.I. (2013). Tectonic development of the Vardar ocean and its margins: Evidence from the Republic of Macedonia and Greek Macedonia. *Tectonophysics*, *595*, 25-54. https://doi.org/10.1016/j.tecto.2012.07.022
[23] Schmid, S.M., Fügenschuh, B., Kounov, A., Matenco, L., Nievergelt, P., Oberhänsli, R., & Van Hinsbergen, D.J. (2020). Tectonic units of the Alpine collision zone between Eastern Alps and western Turkey. *Gondwana Research*, *78*, 308-374. https://doi.org/10.1016/j.gr.2019.07.005
[24] Schmid, S.M., Bernoulli, D., Fügenschuh, B., Matenco, L., Schefer, S., Schuster, R., & Ustaszewski, K. (2008). The Alpine-Carpathian-Dinaridic orogenic system: Correlation and evolution of tectonic units. *Swiss Journal of Geosciences*, *101*(1), 139-183. https://doi.org/10.1007/s00015-008-1247-3
[25] Sinani, B., Boev, B., Reka, A.A., Sinani, B., & Boev, I. (2025). GTMod 1.0: A geological and geotectonic tool for ore body modeling-case study of the Trepça mine. *Earth Science Informatics*, *18*(4), 1-13. https://doi.org/10.1007/s12145-025-02038-x
[26] Karamata, S. (2006). The geological development of the Balkan Peninsula related to the approach, collision and compression of Gondwanan and Eurasian units. *Geological Society, London, Special Publications*, *260*(1), 155-178. https://doi.org/10.1144/GSL.SP.2006.260.01.07
[27] Mehana, Y. (2024). *Research of the presence of heavy metals in drinking water in the villages of Kelmend, Zhazhë, Boletin, Melenicë, Vllahi, Maxherë, Zjaqë*. MSc Thesis. Mitrovicë, Kosovo: University "Isa Boletini".
[28] Elezaj, Z., & Kodra, A. (2008). *Geology of Kosovo*. Pristina, Kosovo: University of Pristina.
[29] State Archives of Kosovo. (2025). *Geological research in Kosovo: Research program for 1980-1981, Geological survey of Yugoslavia*. State Archives of Kosovo. Retrived from: https://katalogu-ashak.net/user-view-search
[30] *Study of Asbestos in Kosovo*. (1973). Pristina, Kosovo: Institute for Geological and Geophysical Research.
[31] Manyama, M.T., Hepelwa, A.S., & Nahonyo, C.L. (2019). Analysis of socio-ecological impacts of built environment at Dar es Salaam Metropolitan Coastline, Tanzania. *Open Journal of Social Sciences*, *7*(10), 161-182. https://doi.org/10.4236/jss.2019.710014
[32] Kruasom, T., Ngeoywijit, S., Sopapol, S., Kosanlawit, T., Sangwarn, S., & Adthajak, P. (2025). From foundations to frontiers: The development and future of structural equation modeling (SEM). *UMT-Poly Journal, 22*(2), 129-149.
[33] Plichko, L.V., Zatserkovnyi, V.I., Khilchevskyi, V.K., Mizernaya, M., & Bakytzhan, A. (2020). Assessment of changes a number of surface water bodies within the sub-basin of the Desna River using remote sensing materials. *Geoinformatics: Theoretical and Applied Aspects*, *1*, 1-5. https://doi.org/10.3997/2214-4609.2020geo101
[34] Shults, R., Soltabayeva, S., Seitkazina, G., Nukarbekova, Z., & Kucherenko, O. (2020). Geospatial monitoring and structural mechanics models: A case study of sports structures. *Environmental Engineering*, *11*, 1-9. https://doi.org/10.3846/enviro.2020.685
[35] Akinboyewa, T., Li, Z., Ning, H., & Lessani, M.N. (2025). GIS copilot: Towards an autonomous GIS agent for spatial analysis. *International Journal of Digital Earth*, *18*(1), 2497489. https://doi.org/10.1080/17538947.2025.2497489
[36] Sadykov, B.B., Baygurin, Zh.D., Altayeva, A.A., Kozhaev, Zh.T., & Stelling, W. (2019). New approach to zone division of surface of the deposit by the degree of sinkhole risk. *Naukovyi Visnyk Natsionalnoho Hirnychoho Universytetu*, *6*, 31-35. https://doi.org/10.29202/nvngu/2019-6/5
[37] Nizamova, A.T., Rasulov, A.K., & Maxmadiyev, D.R. (2025). Assessment of industrial waste disposal practices in the mining sector of Uzbekistan. *Engineering Journal of Satbayev University*, *147*(4), 23-29. https://doi.org/10.51301/ejsu.2025.i4.04
[38] Liu, Q., Liu, G., Chen, W., & Chen, G. (2021). HMCA-contour: A visual basic program based on surfer automation for soil heavy metal spatial distribution and contamination assessment mapping. *Sustainability*, *13*(4), 2282. https://doi.org/10.3390/su13042282
[39] Pour, A.B., Parsa, M., & Eldosouky, A.M. (2023). Introduction to mineral exploration. *Geospatial Analysis Applied to Mineral Exploration*, 1-16. https://doi.org/10.1016/B978-0-323-95608-6.00001-9
[40] Balaram, V., & Subramanyam, K.S.V. (2022). Sample preparation for geochemical analysis: Strategies and significance. *Advances in Sample Preparation*, *1*, 100010. https://doi.org/10.1016/j.sampre.2022.100010
[41] Balaram, V. (2021). Current and emerging analytical techniques for geochemical and geochronological studies. *Geological Journal*, *56*(5), 2300-2359. https://doi.org/10.1002/gj.4005
[42] Park, C.S., Shin, H.S., Oh, H., Cho, H., & Cheong, A.C.S. (2016). Trace element analysis of whole-rock glass beads of geological reference materials by Nd: YAG UV 213 nm LA-ICP-MS. *Journal of Analytical Science and Technology*, *7*(1), 15. https://doi.org/10.1186/s40543-016-0094-5
[43] Ceci, A., Costanza, G., & Tata, M.E. (2025). Microstructural and XRD investigations on Zn after plastic deformation. *Crystals*, *15*(10), 908. https://doi.org/10.3390/cryst15100908
[44] Wicks, F.J., & Whittaker, E.J.W. (1977). Serpentine textures and serpentinization. *The Canadian Mineralogist*, *15*(4), 459-488.
[45] Mellini, M. (2013). *Structure and microstructure of serpentine minerals*. *EMU Notes in Mineralogy*, *14*, 1-27. https://doi.org/10.1180/EMU-notes.14.5
[46] Mellini, M., & Zanazzi, P.F. (1987). Crystal structures of lizardite-1T and lizardite-2H1 from Coli, Italy. *American Mineralogist*, *72*(9-10), 943-948.
[47] Mambetaliyeva, A.R., Mamyrbayeva, K.K., Turysbekov, D.K., Dauletbakov, T.S., & Barmenshinova, M.B. (2022). Investigation of the process of sulfiding of gold-arsenic containing ores and concentrates. *Naukovyi Visnyk Natsionalnoho Hirnychoho Universytetu*, *3*, 51-56. https://doi.org/10.33271/nvngu/2022-3/051
[48] Rinaudo, C., Gastaldi, D., & Belluso, E. (2003). Characterization of chrysotile, antigorite and lizardite by FT-Raman spectroscopy. *The Canadian Mineralogist*, *41*(4), 883-890. https://doi.org/10.2113/gscanmin.41.4.883
[49] Shirokiy, P.G., Zavaley, V.A., Auelkhan, Y.S., & Alzhigitova, M.M. (2024). Application of geostatistical interpolation methods for filtration coefficients on the Nurkazgan East field using the Python programming language. *Engineering Journal of Satbayev University*, *146*(1), 23-29. https://doi.org/10.51301/ejsu.2024.i1.04
[50] Mas'idah, E., & Marlyana, N. (2022). The study of the application of noise mapping using Golden Surfer Software to control noise. *Journal of Applied Science and Technology*, *2*(02), 28-35. https://doi.org/10.30659/jast.2.02.28-35

Еколого-геологічна оцінка природного азбесту на основі мінералогічного та просторового аналізу: район Байгора-Митровиця, Косово

Б. Сінані, Б. Боєв, А. Река, Б. Сінані, І. Боєв

Мета. Оцінити просторовий розподіл і мінералогічну мінливість природного азбесту (NOA) в районі Байгора та визначити його екологічну значущість з урахуванням геологічних умов і сучасного землекористування з метою виділення азбестоносних зон та формування просторової основи для оцінки екологічної небезпеки.

Методика. Дослідження виконано з використанням комплексного мінералогічного, статистичного та геоінформаційного підходу. В процесі дослідження відібрано 20 репрезентативних зразків гірських порід, які проаналізовано методами рентгенофазового аналізу (XRD) і сканувальної електронної мікроскопії з енергодисперсійним аналізом (SEM-EDX) з метою ідентифікації та кількісної оцінки азбестовмісних мінеральних фаз. Для оцінки мінералогічної мінливості та взаємозв'язків між фазами застосовано описо-

ву статистику, кореляційний аналіз і метод головних компонент (PCA). Просторове моделювання розподілу серпентинових мінералів і хризотилу виконано методом крігінгу з використанням ГІС-технологій.

Результати. Встановлено значну мінералогічну неоднорідність району Байгора, з домінуванням мінералів серпентинової групи, зокрема лізардиту (з кількома поліморфними різновидами), антигориту та підпорядкованого хризотилу. Лізардит є найбільш поширеною фазою та пов'язаний з низькотемпературними процесами серпентинізації, тоді як антигорит локально домінує за підвищених температурно-тискових умов. Хризотил має дискретний просторовий розподіл і приурочений до структурно ослаблених зон, тріщинних систем і літологічних контактів. Статистичні та багатовимірні аналізи підтвердили нерівномірний характер розподілу мінеральних фаз і їх жорсткий геологічний контроль.

Наукова новизна. Уперше для району Байгора реалізовано інтегрований підхід, що поєднує детальну мінералогічну характеристику азбестовмісних фаз із просторовим та статистичним аналізом для оцінки екологічної небезпеки в офіолітових комплексах Західних Балкан.

Практична значимість. Побудовані карти просторового розподілу азбестовмісних мінералів можуть бути використані для екологічного зонування території, планування землекористування, організації моніторингу та розробки заходів з мінімізації ризиків для населення і довкілля.

Ключові слова: *природний азбест; хризотил; серпентинові мінерали; просторовий аналіз; екологічна небезпека*

Publisher's note

All claims expressed in this manuscript are solely those of the authors and do not necessarily represent those of their affiliated organizations, or those of the publisher, the editors and the reviewers.